



Heriot-Watt University  
Research Gateway

# Geological feature selection in reservoir modelling and history matching with Multiple Kernel Learning

## Citation for published version:

Demyanov, V, Backhouse, LJ & Christie, MA 2015, 'Geological feature selection in reservoir modelling and history matching with Multiple Kernel Learning', *Computers and Geosciences*, vol. 85, no. Part B, pp. 16-25. <https://doi.org/10.1016/j.cageo.2015.07.014>

## Digital Object Identifier (DOI):

[10.1016/j.cageo.2015.07.014](https://doi.org/10.1016/j.cageo.2015.07.014)

## Link:

[Link to publication record in Heriot-Watt Research Portal](#)

## Document Version:

Peer reviewed version

## Published In:

Computers and Geosciences

## Publisher Rights Statement:

Copyright © 2015 Elsevier Ltd.

## General rights

Copyright for the publications made accessible via Heriot-Watt Research Portal is retained by the author(s) and / or other copyright owners and it is a condition of accessing these publications that users recognise and abide by the legal requirements associated with these rights.

## Take down policy

Heriot-Watt University has made every reasonable effort to ensure that the content in Heriot-Watt Research Portal complies with UK legislation. If you believe that the public display of this file breaches copyright please contact [open.access@hw.ac.uk](mailto:open.access@hw.ac.uk) providing details, and we will remove access to the work immediately and investigate your claim.

1 Geological Feature Selection in Reservoir Modelling and History Matching with Multiple  
2 Kernel Learning.

3 V. Demyanov, L. Backhouse, M. Christie

4 Institute of Petroleum Engineering, Heriot-Watt University, Edinburgh, UK.

5 vasily.demyanov@pet.hw.ac.uk

6 1 Abstract

7 There is a continuous challenge in identifying and propagating geologically realistic features into  
8 reservoir models. Many of the contemporary geostatistical algorithms are limited by various modelling  
9 assumptions, like stationarity or Gaussianity. Another related challenge is to ensure the realistic  
10 geological features introduced into a geomodel are preserved during the model update in history  
11 matching studies, when the model properties are tuned to fit the flow response to production data. The  
12 above challenges motivate exploration and application of other statistical approaches to build and  
13 calibrate reservoir models, in particular, methods based on statistical learning.

14 The paper proposes a novel data driven approach – multiple kernel learning (MKL) – for modelling  
15 porous property distributions in sub-surface reservoirs. Multiple kernel learning aims to extract relevant  
16 spatial features from spatial patterns and to combine them in a non-linear way. This ability allows to  
17 handle multiple geological scenarios, which represent different spatial scales and a range of modelling  
18 concepts/assumptions. Multiple Kernel Learning is not restricted by deterministic or statistical  
19 modelling assumptions and, therefore, is more flexible for modelling heterogeneity at different scales  
20 and integrating data and knowledge.

21 We demonstrate an MKL application to a problem of history matching based on a diverse prior  
22 information embedded into a range of possible geological scenarios. MKL was able to select the most  
23 influential prior geological scenarios and fuse the selected spatial features into a multi-scale property  
24 model. The MKL was applied to Brugge history matching benchmark example by calibrating the  
25 parameters of the MKL reservoir model parameters to production data. The history matching results

26 were compared to the ones obtained from other contemporary approaches – EnKF and kernel PCA with  
27 stochastic optimisation.

28 Keywords: kernel learning, uncertainty quantification, history matching, Brugge case study

## 29 2 Introduction

30 Sub-surface reservoir characterisation is subject to vast uncertainties that make prediction of the  
31 reservoir dynamic behaviour a challenging task, which usually involves history matching to calibrate a  
32 model to dynamic data. Uncertainties in reservoir characterisations are of different kinds: (i) data  
33 uncertainty associated with the observation/calibration errors; (ii) model uncertainty related to the  
34 model description (e.g. assumptions, equations, parameters etc.); (iii) model solution errors subject to  
35 the numerical solver algorithm and discretisation accuracy used (e.g. in O’ Sullivan & Christie, 2005);  
36 (iv) model inadequacy representing the physics missing from the model that can be accounted for by  
37 other means (e.g. after Kennedy & O’Hagan).

38 History matching (HM) of reservoir models to dynamic data provides a way to infer model uncertainty  
39 to make more accurate predictions. Traditionally history matching becomes an exercise in inferring the  
40 model parameter values, that are chosen based on the given model description. Inferring uncertainty  
41 related to geological model description through history matching remains challenging, because it often  
42 needs to be done across a set of model with different parameters and even equations (e.g. Gaussian vs  
43 Boolean).

44 The static model or “geomodel” encapsulates the best understanding of the relationship between  
45 geological and petrophysical parameters based on the geological interpretation, e.g. depositional  
46 environment, selection and description of facies, etc. Geological interpretation is one of the main  
47 uncertainties commonly biased towards a subjective opinion and is often difficult to rigorously quantify  
48 (Bond et al., 2007). Uncertainty from the geological interpretation may often prevail over the  
49 uncertainty coming from the chosen set of the model parameters or the subs-scale variability, the latter  
50 is represented by the stochastic nature (seed) of a geomodelling algorithm. Therefore, it is important to  
51 history match across multiple plausible model descriptions / geological interpretations where relevant.

52 Geostatistical algorithms are traditionally used to describe the distributions of spatial properties in  
53 geomodels. Geostatistical algorithms are good in establishing the appropriate level conditioning to  
54 geological measurement data. A range of stochastic geostatistical algorithms based on a  
55 covariance/variogram function, objects or training images are routinely used to populate the geomodel  
56 grid with lithological and petrophysical properties (Chiles J-P. and Delfiner P. 2009; Mariethoz G.,  
57 Caers J., 2014). All of them involve evaluation of the model dependent parameters: object geometries  
58 and placements in the object-based models; variogram correlation range and anisotropy for Gaussian or  
59 Indicator simulations; training image definition and appropriate local transformation for multipoint  
60 statistics (MPS) models.

61 These parameters are often inferred in a history matching task within the single chosen set of model  
62 equations, e.g. using a single training image or a certain set of object shapes (with limited allowed  
63 transformations). For example, the history matching of the variogram model parameters of a Gaussian  
64 Random Field model description was done through a Bayesian uncertainty quantification framework  
65 (Demyanov et al, 2004). History matching of channelised reservoir training image based models with  
66 realistic prior information was done in (Rojas et al., 2014 a&b). More recently, the challenge in  
67 accounting uncertainty across multiple model definitions in history matching has been tackled in (Park  
68 et al., 2013; Rojas et al., 2013). They considered different geological interpretations with multiple  
69 training images and implements history matching in the distance metric space.

70 Calibration of geostatistical models to dynamic data still remains a challenge for the industry, though a  
71 lot of research has been done in developing history matching techniques that include gradual  
72 deformation method (GDM) (Hu, 2000); probability perturbation approach (Caers, Hoffman, 2006),  
73 which extends GDM to probabilistic Bayesian formulation; adaptation of population based stochastic  
74 optimisation algorithms (Mohamed et al., 2010, Schulze-Riegert et al., 2002), other gradient based  
75 approaches for this problem (Gomez et al., 2001; Bissel et al, 1997).

76 Among other approaches, emerged more recently, there is a pattern based history matching with multi-  
77 point statistics facies modelling in (Melnikova, et al., 2015), where spatial probabilistic information is  
78 elicited from training images and then inferred in a Bayesian way. Ensemble based data assimilation

79 approach, such as EnKF, have been also widely used to evaluate uncertainty with an ensemble of  
80 calibrated models (Evensen, 1998). Ensemble based approaches have an advantageous capability of  
81 more flexible integration of prior knowledge – in a form of initial prior set of models, which are  
82 gradually assimilated through perturbation of the model state to fit the observed dynamic response.  
83 Such setting is suitable to account for multiple possible prior model states, which represent uncertainty  
84 in geological reservoir description (e.g. as in Peters 2008). However, preserving geological realism in the  
85 posterior ensemble still remains a challenge. Several history matching studies have been performed  
86 following this approach (Oliver et al, 2011; Chen et al 2010; Mohamed et al, 2010 a). Clustering across  
87 an ensemble of geological realisations was implemented in adaptive sparse model representation in a  
88 history matching study by Khaninezhad and Jafapour, 2014.

89 In this paper we propose a way to history match a reservoir model across different possible prior  
90 geological scenarios (model descriptions). We use a data driven kernel based model to populate  
91 petrophysical reservoir properties to integrate multiple types of data: observed data from wells, soft  
92 seismic information and multiple geological concepts (prior ensemble). Multiple Kernel Learning  
93 (MKL) model selects relevant spatial features from multi-scale input information. The MKL model is  
94 then history matched to production data using adaptive stochastic sampling (particle swarm  
95 optimisation).

## 96 3 Modelling Approaches

### 97 3.1 Data integration in reservoir modelling

98 Traditional geostatistics have been used for efficient data integration in reservoir modelling.  
99 Geostatistical paradigm allows integrating point and pattern data through model conditioning to data  
100 with a linear regression under a two-point covariance spatial relationship. Secondary (soft) correlated  
101 information can be integrated through a linear relation, e.g. kriging with external drift (Chiles and  
102 Delfiner, 1999) or collocated co-kriging (Almeida & Journel, 1994), see Annex for more details.

103 More recently multipoint statistical moments have been implemented in geostatistical prediction  
104 (Strebelle, 2002; Dimitrakopoulos, 2010) to extend the flexibility of spatial correlation model beyond  
105 the two-point covariance. Multi-point statistics approach is superior to a classical two-point statistics,  
106 because it provides a richer, more flexible and a generalised description of spatial correlation  
107 (Mariethoz G., Caers J., 2014), see Annex for more details. However, it is still subject to the stationarity  
108 assumption of some form (training image) and it has a limited linear capacity in integrating multivariate  
109 and multi-scale secondary information (Strebelle et al., 2005; Hu et al, 2008). The problem of non-  
110 stationarity is often addressed through accounting for a trend, which usually implies a linear relation  
111 with the simulated probability field. A more recent pattern simulation algorithm, which handles non-  
112 stationary training images using a distance metric approach, was proposed in (Honarkhah & Caers,  
113 2012).

114 In the present work we will address the problem of improving the flexibility of spatial reservoir  
115 property model description with a non-linear integration of spatial information from multiple patterns,  
116 which represent possible geological concepts. This approach provides more flexibility in data  
117 conditioning within a statistical learning paradigm and is not restricted by stationary assumptions, since  
118 it is purely data driven.

### 119 3.2 Statistical learning in reservoir modelling

120 In recent years statistical learning (Vapnik 1995) has become more intensively used for modelling  
121 geological reservoir properties. Data driven algorithms have shown to be an efficient alternative to  
122 traditional modelling approaches for difficult problems, e.g. dealing with noisy data or non-stationary  
123 cases. Kernel learning methods – Kernel PCA, Support Vector Machines (SVM), Multiple Kernel  
124 Learning (MKL) –have been applied for modelling and classification of reservoir properties (Sarma, et  
125 al. 2008; Demyanov, et al. 2008, 2011; Alanazi 2009). Kernel based methods have been also used for  
126 multi-dimensional scaling of model realisations into the metric space for more representative ranking  
127 and description of relations between different geological scenarios (Scheidt & Caers, 2009).

128 In earlier work (Demyanov, et al. 2008) we have demonstrated capabilities of the semi-supervised  
129 Support Vector Regression (SVR) to successfully model petrophysical property distributions in a fluvial  
130 reservoir. SVR model computes linear regression in high dimensional space (the reproducing kernel  
131 Hilbert space) using a single kernel for implicit mapping of the data. However, a single kernel makes it  
132 difficult to reproduce multi-scale non-stationary spatial patterns. The difficulty was partly overcome by  
133 using semi-supervised learning approach with unlabelled data, which, however, does not explicitly  
134 reflect the correlation on multiple scales. The Multiple Kernel Learning (MKL) model applied in this  
135 paper is a generalisation of SVR that allows multiple kernel representation for every separate model  
136 input. For instance, when modelling a gridded porosity distribution conditioned to core data from wells  
137 and seismic, separate kernels will be used for spatial co-ordinates and the soft multi-component seismic  
138 input to account for information at different scales (well scale, seismic components). Thus, MKL  
139 provides capability to rigorously integrate different multi-scale information, which represents various  
140 geologically relevant features. For instance, MKL was applied for modelling spatial wind fields in  
141 Foresti, et al. 2011. Demyanov et al. (2011) used MKL to select relevant spatial scales derived from  
142 seismic in a history matching study.

143 In the present work we extend MKL application in reservoir modelling in attempt to integrate spatial  
144 information from multiple possible geological scenarios. MKL based geomodel framed in a history  
145 matching context aims to select spatial features from those geological scenarios that are more likely to  
146 support production data.

### 147 3.3 Feature selection in History Matching Workflow with Multiple Kernel Learning

148 Feature (or variable) selection is the technique whereby a subset of variables is chosen from the  
149 available set. This subset includes those variables most relevant in predicting the response or outcome.  
150 Feature selection applied for geomodelling allows extracting the most relevant information from the  
151 input data and creating a multitude of possible geological realisations previously not available.

152 One of the principle problems in reservoir modelling is to describe the relations between the observed  
153 spatial information and the target predicted variables – porosity and permeability. These relations are

154 highly complex and subject to many uncertainties. The group of all possible geological scenarios along  
155 with all other available information, such as seismic, outcrop, etc., are known as variables used in  
156 reservoir description. The problem is to which extent a model needs to be conditioned to each piece of  
157 data and how to relate different bits of the data within the model in the most relevant and geologically  
158 plausible way. We have already mentioned that among the limitations of geostatistics are hard kriging  
159 conditioning under stationarity and linear relations with soft conditioning information. MKL, as a data  
160 driven approach, is capable of finding dependencies embedded in the input geological features and  
161 integrating them into the spatial property prediction model through a non-linear weighting. For instance,  
162 in case of seismic, which is commonly used as soft conditioning data in geostatistical modelling, the  
163 challenge is to determine the influence seismic data have on the prediction of porous properties.

164 MKL shows distinct advantages over competing methodologies such as Kernel PCA and EnKF. The  
165 weights assigned to each feature in MKL are interpretable in that they sum to one. From this one can  
166 ascertain those variables that are the most important in the prediction as well as those that are  
167 redundant. The weight is applicable to each input variable or feature and not to some mapped or  
168 transformed variable as it is in Kernel PCA. A further disadvantage of KPCA is that the output suffers  
169 from the supposed “pre-image” problem. That is the output has to be inversed mapped into the input  
170 space that is usually far larger than the mode response output space due to the nature of the inverse  
171 problem (Bakır et al., 2004).

172 Feature selection is carried out by means of an optimisation through a training process (see Figure 1).  
173 MKL computes prediction of the target variable with the selected features, unlike other machine  
174 learning algorithms (e.g. artificial neural networks), where the feature selection (choice of inputs) is a  
175 pre-conditioning step applied prior to training the algorithm. Tsamardinos et. al (2003) pointed out that  
176 the selection of the relevant features may well be a subset rather than individual features. That is, a  
177 group of features are selected together to produce the MKL prediction. Different combinations of  
178 selected features identify a range of model description scenarios driven by data rather than by pre-  
179 defined fixed assumptions.



180 MKL has the advantage of being efficient in that feature selection is not a process carried out either  
181 before or after the training. MKL is efficient as a feature selection technique in that relevant features are  
182 selected automatically in the tuning of the parameters stage. This is unlike other methods where feature  
183 selection is performed first then the estimation model is run.

184 In this paper we will use a dual loop to tune MKL reservoir model for porosity ( $\phi$ ) and permeability ( $k$ ):  
185 (i) the inner loop optimises the impact of the input features by minimising the mismatch of the static  
186 model; (ii) the outer loop tunes MKL hyper-parameters to minimise the dynamic mismatch of the  
187 reservoir model response (see Figure 1). We will also discuss the differentiation in the impact of the  
188 input features, which represent prior geological scenarios.

189 **FIGURE 1 HERE**

190 MKL has been used as a feature selection technique in various diverse applications: Tuia, D., et. al.  
191 (2010) applied MKL to select relevant features from satellite images; Takashima et al. (2011) applied  
192 MKL to select the relevant spectral dimension of the acoustic transfer function in sound source  
193 localization; Dileep et. al. (2009) details the theory of MKL feature selection and applied it to an image  
194 classification problem.

195 The data driven MKL predictor is still subject to the choice of the parameter values, which define the  
196 kernels for each input feature ( $\sigma_i$ ), the complexity bound  $C$  on the support vectors and the error margin  $\varepsilon$   
197 (for more details on the support vector regression refer to section 4.1 and Figure 3). Ad-hoc trial and  
198 error choice of these most influential parameters may be quite risky. He et al. (2008) used a genetic  
199 algorithm to tune the parameters of their feature selection algorithm MO-SVR iteratively analysing the  
200 scale of each factor ( $\sigma$  of the Gaussian Kernel). Kanevski et al. 2009 and Foresti, 2011 followed a cross-  
201 validation/testing approach in picking optimal combination of kernel parameters from the test error  
202 surface.

203 In this work we use a history matching loop to tune the MKL model parameters ( $\sigma_i$ ,  $C$ ,  $\varepsilon$ ) using particle  
204 swarm optimisation (PSO, Kennedy & Eberhart, 1995) (see Figure 1). This includes populating  
205 reservoir grid with porosity ( $\phi$ ) and permeability ( $k$ ) and the subsequent flow simulation to compute the

206 dynamic model response. MKL model parameters are updated iteratively guided by the mismatch  
207 between the history and the dynamic model response. The MKL prediction model is then re-trained to  
208 update the feature selection (through the weights  $w_i$ ) with every update in its parameters.

## 209 4 Theory of the algorithms

210 This section overviews kernel learning algorithms applied for porosity/permeability field prediction.  
211 First, we briefly overview support vector regression, for which MKL is a generalisation.

### 212 4.1 Support Vector Regression (SVR)

213 Support vector regression (SVR) is a function estimation extension of the well-known support vector  
214 machine classifier developed within the framework of the statistical learning theory (Vapnik, 1995). By  
215 controlling model complexity SVR provides robust solutions to non-linear and high-dimensional  
216 regression problems.

217 SVR belongs to the family of kernel methods that allow finding linear solutions to non-linear regression  
218 problems by applying an implicit Hilbert space mapping to original input data. Such mapping is carried  
219 out by means of kernel functions. Kernels can be used to replace dot products between training points in  
220 a higher dimensional (Hilbert) space, where the original data are mapped. More formally, the so called  
221 "kernel trick" can be defined as

$$222 \quad K(\mathbf{x}, \mathbf{x}_i) = \psi(\mathbf{x}) \cdot \psi(\mathbf{x}_i) \quad (1)$$

223 where  $\psi$  denotes the mapping of an input vector  $\mathbf{x}$  to the Hilbert space. Among the broad list of  
224 kernels which have been tested in different studies (Kanevski et al. 2009), we have chosen a Gaussian  
225 RBF kernel for this paper.

226 SVR prediction at  $\mathbf{x}$  becomes as a weighted expansion of kernels (Schölkopf and Smola, 2002):

$$227 \quad f(\vec{x}) = \sum_{i=1}^{N_{sv}} \alpha_i K(\mathbf{x}, \mathbf{x}_i; \theta) + b \quad (2)$$

228 where  $\alpha_i$  are Lagrangean multipliers,  $K(\mathbf{x}, \mathbf{x}_i; \theta)$  is the kernel function with its internal hyper-  
229 parameters  $\theta$ ,  $b$  is the bias and  $N_{sv}$  is the number of support vectors.

230 A key component of the SVR model formulation is the definition of an a-priori level of noise in the data  
231 as can be seen in Figure 2. Such robust cost function, also called " $\varepsilon$ -tube" defined by the hyper  
232 parameter  $\varepsilon$ , allows building sparse models using only a reduced set of the data (called support  
233 vectors). The amount of noise assumed is controlled by the parameter  $\varepsilon$ . The amount of penalisation for  
234 the data lying outside the  $\varepsilon$ -tube is controlled by the parameter  $C$ , which is the bound for the support  
235 vectors. The data points which lie outside the  $\varepsilon$ -tube are penalised according to a free complexity  
236 parameter  $C$  yielding a regularized solution.

237

**FIGURE 2 HERE**

## 238 4.2 Multiple Kernel Learning (MKL)

239 MKL predictor can be written in a non-linear kernel form:

$$240 \quad Z(x) = \sum_{m=1}^P w_m \sum_{i=1}^{N_{sv}} \alpha_i K_m(\mathbf{x}, \mathbf{x}_i, \sigma_m, C, \varepsilon) \quad (3)$$

241 where  $\sigma_m$  denotes the internal parameter of the single kernel and  $w_m$  its respective weight.

242 Thus, a multiple kernel forms a weighted convex combination of  $m$  basis kernels. The regression eq. 3  
243 is similar in some way to the kriging equation (see Annex eq. A.1), further more  $w_m$  sum to 1, but are  
244 also positive definite (Lanckriet et al., 2004). The principle difference is that the linear kriging  
245 regression weighs the outputs – the observed values of the target variable  $Z(\mathbf{x}_i)$ ; while MKL is a  
246 regression of the inputs in the kernel form  $K(\mathbf{x}, \mathbf{x}_i)$ . This is provided through implicit mapping of data  
247 points from the input space to a reproducing kernel Hilbert space (RKHS). The resulting space induced  
248 by the multiple kernel is the sum of all RKHS for which the weights  $w_m$ 's are non-zero (feature  
249 selection). The kernels introduce a non-linear element and correspond to the support vectors  $\alpha_i$ , which  
250 are determined for each input feature through training. Impact of the relevant features is controlled by  
251 the weights  $w_m$ , i.e. the selected features get higher weighting. The optimal weighted combination can

252 give insights about the relevance of the input features/kernels. The multiple kernel formulation brings a  
253 lot of flexibility by handling a variety of input features and kernel hyper-parameter tuning. A multi-  
254 scale processes can be modelled by using two or more kernels of different bandwidths  $\sigma_m$  acting on the  
255 same input feature (Pozdnoukhov et al., 2008). Data integration can be approached by considering one  
256 kernel for each source of information (e.g. Demyanov et al., 2011).

257 Several algorithms have been proposed to solve the MKL problem efficiently, i.e. to find the optimal  
258 weighted combination (Lanckriet, et al., 2004; Sonnenburg, et al., 2006). In this paper we used  
259 SimpleMKL algorithm proposed by Rakotomamonjy et al., 2008, where the convex problem is solved  
260 with a dual loop optimisation through gradient with line search and descent direction update  
261 (implemented in the inner loop in Fig. 1). In this work we have applied a Simple MKL implemented in  
262 the similar way as in (e.g. Demyanov et al., 2011):

### 263 **Table 1. MKL Algorithm**

264

---

265 initialise MKL parameters  $C$  and  $\sigma$  for each kernel for both porosity and permeability models within  
266 prior ranges

267 **repeat**

- 268 – train MKL with the given parameters and predict porosity (Feature selection loop in Fig. 1)
- 269 – add the predicted porosity to the chosen input features, re-train MKL to predict permeability
- 270 – run flow simulation on the reservoir reservoir grid populated with porosity and permeability  
271 and forecast oil production from the
- 272 – compute misfit w.r.t. to historical oil production data for each of the 20 production wells
- 273 – update  $C$ ,  $\varepsilon$  and kernel widths  $\sigma$  by adaptive stochastic sampling from the prior

274 **until** convergence of parameters and matching of oil/water production (observed at 500 iterations)

275

---

## 276 5 History Matching with MKL Reservoir Model

### 277 5.1 Brugge Reservoir Case Study Description

278 Feature selection problem was formulated for Brugge reservoir model. Brugge case study was designed  
279 as a benchmark problem for history matching and optimisation (Geel, 2008; Peters et al., 2010). The  
280 reservoir consists of four stratigraphic zones: fluvial (deltaic), lower shore face, upper shore face and  
281 sandy shelf (Geel, 2008). The unique characteristic of this model is the provided prior ensemble of grids

282 of the porous properties, which represent the spread of geological uncertainty according to the initial  
283 beliefs about the reservoir geology. The prior ensemble of 104 unconditional realisations designed by  
284 TNO includes the models that are described by different geostatistical algorithms (objects based and  
285 variogram based) and with variable assumptions about the facies and properties correlations (Geel,  
286 2008). Prior realisations (Fig. 3, sand shelf layer shown only) do not match the production data, which  
287 sets up a history matching challenge.

288

### FIGURE 3 HERE

289 Stratigraphy of Brugge reservoir includes four zones (split into 9 grid layers), which represent a typical  
290 sequence of depositional environments in a Brent reservoir: fluvial, lower shoreface, upper shoreface  
291 and a sandy shelf. Each layer features its own spatial structure, correlation of porosity and permeability  
292 and their statistical distribution properties.

## 293 5.2 MKL reservoir property model

294 Feature selection with MKL aims to select the most relevant geological features from the ensemble of  
295 prior realisations based on how well the combination of these features fit the observed well data and  
296 match the production history. MKL is capable of non-linear blending of the selected spatial features to  
297 provide the right balance of each bit of the input data (from the wells) and weigh their impact on the  
298 property distribution at a distance.

299 MKL was applied to predict porosity ( $\varphi$ ) and permeability ( $k$ ) fields from the input features following  
300 the workflow in Fig. 1 and the training algorithm (see Table 1). MKL was trained using the target  
301 (output) on porosity and permeability data from 30 well locations interpreted from the wireline logs,  
302 which slightly vary from the properties observed across the prior ensemble of 104 realisations. The  
303 gridded porosity and permeability from the prior realisations were used as the inputs for the MKL  
304 model. In case of the permeability predictor – the modelled porosity was used as an additional input to  
305 establish the petrophysical correlation between the two properties derived from the data. Seismic data  
306 (4D) as pressure and saturation differences (see Fig. 4) were used as additional inputs. Separate MKL  
307 models were defined for each of the four stratigraphic zones corresponding to the different depositional

308 environments: fluvial (2 grid layers), lower shore face (3 grid layers), upped shore face (3 grid layers)  
309 and sandy shelf (1 layer). This makes altogether 8 MKL predictors for  $\varphi$  and  $k$ . Kernel transformation  
310 of the input features in to porosity and permeability fields by the MKL predictor is schematically  
311 illustrated in Fig. 5. Figure 6 illustrates MKL porosity models computed with different hyper-parameter  
312 values.

313 **FIGURE 4 HERE**

314 **FIGURE 5 HERE**

315 **FIGURE 6 HERE**

### 316 5.3 History Matching Model set-up

317 The history matching challenge has been tackled in many studies using different approaches (Peters et  
318 al., 2010). Although, the Brugge benchmark was very suitably designed for EnKF application, a  
319 comparative study (Mohamed et al., 2010b) found that history matching with Particle Swarm  
320 optimisation (PSO) was able to provide matches of equally good quality as the EnKF ones but different  
321 between each other.

322 History matching of Brugge model often requires re-parametrisation of the geological property  
323 distribution to introduce a common metric for the prior realisations, for instance kernel PCA was  
324 implemented in (Mohamed et al, 2010 b). This can be seen as a potential weakness as the realisations  
325 evolved through history matching may lose geological realism and consistency with the prior geological  
326 assumptions. Keeping the updated model realisations within the geological prior is not a straightforward  
327 problem once it comes to patterns and uncertainty in geological model description. An approach for  
328 eliciting prior information from patterns was proposed in (K. Lange, et al. , 2012), where the prior pdf  
329 of patterns elicited from a training images was inferred. This is a plausible approach, however,  
330 questions still remain: how much information is there in the a priori training image to elicit and what are  
331 the means by which it should be elicited in the most effective way.

332 This paper attempts to find some answers through the kernel learning route. So, it is for the data to  
333 prompt how much and what kind of information is to be inferred from the prior into the posterior. We  
334 have sampled the MKL parameters from the prior. We have checked that the generated models are  
335 consistent with the spatial correlation structures reflected in the prior patterns (which is some  
336 representation of the a priori). MKL hyper-parameters require tuning, which was done through history  
337 matching to calibrate the reservoir model flow response to production data. The historical data from the  
338 past 10 years were used in to calibrate the MKL property model in an inverse loop (similar to  
339 Demyanov et.al. 2011, where a Neighbourhood approximation was used). The least square misfit  
340 between the flow simulation response and the historical production (pressure and rates at the individual  
341 wells) ranked the match quality and drove the history matching process (after Mohamed et al. 2010b).

342 In this work we used Particle Swarm Optimisation algorithm (PSO, after Kennedy & Eberhart 1995)  
343 sample iteratively from the prior uniform ranges of the MKL hyper-parameters parameters: kernel  
344 bandwidth for each input feature  $\sigma_i$ , regularisation constant  $C$  and error margin  $\varepsilon$  (see the outer loop in  
345 Fig. 1). The prior intervals for the kernel bandwidths  $\sigma_i$  were defined as a fraction of the corresponding  
346 feature range. The prior interval for the regularisation parameter  $C$ , which controls the roughness of the  
347 predictions, was chosen according to the uncertainty of the maximum value for the predicted property.

348 MKL predictions of porosity and permeability reservoir grids computed for every combination of the  
349 kernel parameters were then the flow simulated (see Fig. 1). The evolution of the MKL kernel  
350 parameters through history matching iterations is illustrated in Fig. 7, where the models with lower  
351 misfit tend to home in around the particular bandwidth values corresponding to the better history match  
352 models. These clusters of models are different for the four reservoir zones of the Brugge reservoir.

353

### **FIGURE 7 HERE**

354 Sampling for the optimal MKL parameters has resulted in a fairly good history match on both field  
355 level and some of the individual wells (see Fig. 8 a,b). The best match was obtained after 2000  
356 iterations and a number of low misfit models were generated for consecutive iterations (Fig. 8c).  
357 Multiple history matches obtained as a result of the stochastic PSO algorithm provide a spread of

358 uncertainty in the production response. PSO set up was chosen to balance the exploration and  
359 exploitation components in HM model search according to earlier studies (Mohammed 2010a). There  
360 were 20 particles with cognitive and social component multipliers equal to 1.333 and inertia decay rate  
361 of 0.9. Each HM run was taken through 3000 iterations that included an MKL call and a flow  
362 simulation each. The CPU time for one 3000 iterations run was 45 h on a 10 node Xeon cluster.

363 The lowest misfit for the best history match achieved was around 180,000, which is better than the  
364 misfit of around 300,000 thousands obtained with kernel PCA model in (Mohamed et al, 2010b). Figure  
365 9 compares the quality of the misfit in the individual wells with the earlier results from Mohamed et al,  
366 2010b). It is clear that various methods result in comparative quality match, however, the match quality  
367 obtained by one or another method differs from one well to another.

368 The use of 4D seismic data (saturation and pressure differences) as two additional MKL inputs  
369 improved was quite important the porosity & permeability predictors. It resulted in taking the history  
370 match misfit down by 50% vs using just the 104 prior geological realisations as the input. The weight of  
371 the seismic features was a few %, which was comparable to the weight of the selected features,  
372 although would vary from one model to another.

373 **FIGURE 8 HERE**

374 **FIGURE 9 HERE**

## 375 6 Results of MKL Feature Selection

376 Feature selection with MKL demonstrated that not all out of the 104 input realisations contributed  
377 equally to the property prediction. The MKL weights  $w_m$  from eq. (3) determine the contribution of  
378 each input feature  $x$ . There were, usually, no more than a dozen of input features that contribute in total  
379 over 90% of the weighting. An example distribution of the weights with the corresponding input  
380 realisations is illustrated in Fig. 10.



381

**FIGURE 10 HERE**

382

**FIGURE 11 HERE**

383 Further investigation of the selected input features revealed that they correspond to different modelling  
384 algorithms and facies assumptions. It appeared that each of the selected features represent a particular  
385 spatial scale from 500 m to 4000 m (see Fig. 11) and their weighting demonstrates a fair spread across  
386 the scale coverage. This leads to an important conclusion about MKL being capable to select multi-  
387 scale information from patterns and then to blend it together in the prediction. Spatial correlation  
388 analysis using variograms illustrates quite complex and multi-scale character of the spatial geological  
389 patterns selected to be blended in the MKL regression model (see Fig. 12). Three out of the seven  
390 selected realisations feature anisotropic spatial correlation with the range (geometric) anisotropy. The  
391 total weight of the anisotropic input realisations contributes to over 30% (see Fig. 12) with the rest  
392 selected inputs being isotropic.

393

**FIGURE 12 HERE**

394 MKL reservoir model calibration in stochastic history matching framework results in multiple good  
395 fitting solution. These solutions are non-unique due to the stochastic nature of the history matching  
396 algorithm (PSO). Therefore, different combinations of input features (and consequently the kernel  
397 algorithm parameters) provide similar quality matches. It was noticed that some of the input realisations  
398 had been repeatedly selected in multiple history matching runs. However, their weights determined  
399 through the MKL training process vary from one history match model to another. Figure 14 illustrates  
400 the variation of the weighting factors for the three most often selected input realisations across 20  
401 history matching runs. Solutions from multiple history matching runs provide the robustness of the  
402 uncertainty spread in the production predictions. **FIGURE 13 HERE**

## 403 7 Conclusions

404 The paper demonstrates an application of multiple kernel learning (MKL) to the problem of selecting  
405 of relevant geological features to describe geological uncertainty in a reservoir history matching study.  
406 MKL proved to be an efficient tool for modelling complex spatial distributions of reservoir properties

407 (porosity and permeability) with a non-linear and multi-scale character. MKL can be seen  
408 complimentary and even advantageous to certain extent to traditional geostatistical algorithms for its  
409 flexibility in integration of diverse spatial multivariate information. However, geostatistical tools are  
410 still needed for modelling geologically realistic input features for MKL. MKL provides a rigorous  
411 balance between fitting a kernel regression model to data, which are subject to noise and possible  
412 interpretational uncertainty, and the model complexity. Model complexity is controlled with the support  
413 vector formalism described by statistical learning theory (Vapnik, 1995).

414 MKL reservoir model is applied to a history matching problem in Brugge case study. Geological  
415 uncertainty is described by a set of prior realisations, which represent a range of different geological  
416 model descriptions based on the algorithmic and the model assumption choices. MKL does not assume  
417 any particular geological description but rather selects relevant spatial patterns based on the available  
418 data through training.

419 MKL reservoir model history matched with PSO resulted in a number models fitted to the production  
420 history. The obtained match quality is comparable or superior to the ones from the previous studies,  
421 where different model parameterisations were used with EnKF or Kernel PCA (Mohamed, 2008b).  
422 History matching with MKL demonstrated that relevant geological patterns were selected from the  
423 ensemble of prior realisations and then blended with the kernel regression in RKHS space to predict  
424 target petrophysical properties. The selected features (geological realisations) represent different spatial  
425 scales and pattern anisotropy. The resulting blends of these patterns provide solutions that match  
426 production data.

## 427 8 Acknowledgment

428 Funding for this work was provided by the industrial sponsors of the Heriot-Watt Uncertainty JIP  
429 (Phase IV). Brugge case study data was supplied by TNO. Foundation Herbette provided funding to  
430 visit University of Lausanne in conjunction to finalising this work.

431 Authors thank Mikhail Kanevski (University of Lausanne) and Dan Arnold (Heriot-Watt) for fruitful  
432 discussions and comments on the work, and Loris Foresti (University of Lausanne) for providing the

433 MKL code. Authors also appreciate the comments from the two anonymous reviewers that helped to  
434 improve the paper.

## 435 9 References

- 436 1. Al-Anazi, A. F., Gates I. D. 2010. "Support vector regression for porosity prediction in a  
437 heterogeneous reservoir: A comparative study." *Computers & Geosciences* 36.12: 1494-1503.
- 438 2. Almeida AS, Journel AG. 1994. "Joint simulation of multiple variables with a Markov-type  
439 coregionalization model". *Math Geology*, 26:565–588.
- 440 3. Bakır, G., Weston, J., & Schölkopf, B. 2004. "Learning to find pre-images". *Advances in Neural  
441 Information Processing Systems*, 16, 449-456.
- 442 4. Bissell, R. C., Dubrule, O., Lamy, P., Swaby, P., & Lepine, O. 1997. "Combining geostatistical  
443 modelling with gradient information for history matching: the pilot point method". In *SPE Annual  
444 Technical Conference and Exhibition*. Society of Petroleum Engineers.
- 445 5. Bond, C. E., Gibbs A.D., Shipton, Z.K., Jones, S. (2007). "What do you think this is? ``Conceptual  
446 uncertainty" in geoscience interpretation". *GSA today* 17.11: 4.
- 447 6. Caers, J. and Hoffman, T. 2006. "The probability perturbation method: a new look at Bayesian  
448 inverse modelling", *Mathematical geology*, 38(1), 81-100.
- 449 7. Chen C., Wang Y., G Li, Reynolds AC. 2010. "Closed-loop reservoir management on the Brugge  
450 test case", *Computational Geosciences*, Volume 14, Issue 4, pp 691-703
- 451 8. Chiles J-P. and Delfiner P. 2009. "Geostatistics: modeling spatial uncertainty". Vol. 497. John  
452 Wiley & Sons.
- 453 9. Demyanov, V., Pozdnoukhov, A., Kanevski, M. and Christie, M. 2008. "Geomodelling of a Fluvial  
454 System with Semi-Supervised Support Vector Regression", *Proceedings of the VII International  
455 Geostatistics Congress, GECAMIN, Chile*, pp. 627-636.

- 456 10. Demyanov V., Foresti L., Christie M. and Kanevski M. 2011. "Reservoir modelling with feature  
457 selection: a kernel learning approach". In Society of Petroleum Engineers Reservoir Simulation  
458 Symposium, 141510-MS, pp. 503-514.
- 459 11. Dimitrakopoulos R., Mustapha H., Gloaguen E. 2010. "High-order Statistics of Spatial Random  
460 Fields: Exploring Spatial Cumulants for Modeling Complex Non-Gaussian and Non-linear  
461 Phenomena", *Math Geosciences*, 42: 65–99.
- 462 12. Dileep, A. D. and Sekhar, C.C. 2009. "Representation and feature selection using multiple kernel  
463 learning". International Joint Conference on Neural Networks. IJCNN 2009. IEEE.
- 464 13. Foresti L. 2011. "Kernel-based mapping of meteorological fields in complex orography", PhD  
465 thesis, University of Lausanne.
- 466 14. Foresti, L., Tuia, D., Kanevski, M. and Pozdnoukhov, A. 2011. "Learning wind fields with multiple  
467 kernels". *Stochastic Environmental Research and Risk Assessment*, 25:51-66.
- 468 15. Geel, K. 2008. "Description of the Brugge field and property realisations, white paper for the  
469 Comparative Case Study on Closed-loop Reservoir Management", SPE ATW on Closed-loop  
470 Reservoir Management, Bruges, Belgium.
- 471 16. Bakır, G.H., Weston, J. and Scholkopf, B. 2004. "Learning to Find Pre-Images", NIPS papers.
- 472 17. Gomez, S., Gosselin, O., & Barker, J. W. 2001. "Gradient-based history matching with a global  
473 optimization method". *SPE Journal*, 6(02), 200-208.
- 474 18. Honarkhah, M., & Caers, J. 2012. "Direct Pattern-Based Simulation of Non-stationary  
475 Geostatistical Models", *Mathematical Geosciences*, 44(6), 651-672.
- 476 19. Hu, L.Y. 2000. "Gradual deformation and iterative calibration of Gaussian-related stochastic  
477 models", *Mathematical Geology*, 32(1), 87-108.
- 478 20. Hu, L. Y., & Chuginova, T. 2008. "Multiple-point geostatistics for modeling subsurface  
479 heterogeneity: A comprehensive review". *Water Resources Research*, 44(11).

- 480 21. Kanevski, M., Pozdnoukhov, A., Timonin, V. 2009. "Machine Learning for Spatial Environmental  
481 Data: theory, applications and software", EFPL Press.
- 482 22. Khaninezhad M.M., Jafarpour B. 2014. "Prior model identification during subsurface flow data  
483 integration with adaptive sparse representation techniques", *Computational Geosciences*, 18 (1), pp  
484 3-16
- 485 23. Kennedy, J., and Eberhart, R. 1995. "Particle swarm optimization", In: *Proceedings of the IEEE*  
486 *International Conference on Neural Networks*, IEEE Service Centre, 4, 1942–1948,
- 487 24. Lanckriet, G. R. G.; Cristianini, N.; Bartlett, P. L.; Ghaoui, L. E.; and Jordan, M. I. 2004. "Learning  
488 the kernel matrix with semidefinite programming", *Journal of Machine Learning Research* 5:27–72.
- 489 25. Lange K., Frydendall J., Cordua K.S., Hansen T.M, Melnikova Y., Mosegaard K. 2012. "A  
490 Frequency Matching Method: Solving Inverse Problems by Use of Geologically Realistic Prior  
491 Information", *Mathematical Geosciences*, 44:783–803.
- 492 26. Mariethoz G, Caers J 2014 . "Multiple-point Geostatistics: Stochastic Modeling with Training  
493 Images", Wiley.
- 494 27. Matheron, Georges 1969. "Part 1 of Cahiers du Centre de morphologie mathématique de  
495 Fontainebleau". *Le krigeage universel*. École nationale supérieure des mines de Paris.
- 496 28. Massonnat, G.J. 2000. "Can we sample the complete Geological Uncertainty Space in  
497 Reservoir Modelling Uncertainty Estimates?" *SPE 38746, SPE Journal*, 5 (1): 46-59.
- 498 29. Melnikova, Y., Zunino, A., Lange, K., Cordua, K.S., Mosegaard, K. 2015. "History Matching  
499 Through a Smooth Formulation of Multiple-Point Statistics", *Mathematical Geosciences*, 47(4),  
500 397-416.
- 501 30. Mohamed, L., Christie, M., Demyanov, V. 2010 a. "Comparison of stochastic sampling algorithms  
502 for uncertainty quantification". *SPE Journal* 15 (01), 31-38.

- 503 31. Mohamed, L., Christie, M., Demyanov, V., Robert, E., and Kachuma, D. 2010 b. “Application of  
504 particle swarms for history matching in the Brugge reservoir”. In: Proceedings of the SPE Annual  
505 Technical Conference and Exhibition (ATCE), SPE 135264.
- 506 32. Oliver, D.S., Chen, Y. 2011. “Recent progress on reservoir history matching: a review,  
507 Computational Geosciences, 15: 185-221.
- 508 33. Park, H., Celine, C., Fenwick, D., Boucher, A. and Caers, J. (2013). “History matching and  
509 uncertainty quantification of facies models with multiple geological interpretation”, Computational  
510 Geosciences, 17 (4), 609-621.
- 511 34. Peters, E., Arts, R., Brouwer, G., and Geel, C. 2010. “Results of the Brugge benchmark study for  
512 flooding optimisation and history matching”. SPE Reservoir Evaluation & Engineering, SPE  
513 119094-PA, 13(3), 391-405.
- 514 35. Pozdnoukhov, A., Kanevski, M. 2008. “Multi-Scale Support vector Regression for hot spot  
515 detection and modeling”, Stochastic Environmental Research and Risk Assessment, 22, 647-660.
- 516 36. Rakotomamonjy, A.; Bach, F. R.; Canu, S.; and Grandvalet, Y. 2008. “SimpleMKL”. Journal of  
517 Machine Learning Research, 9:2491-2521.
- 518 37. Rojas, T.A., Demyanov, V., Christie, M., Arnold, D. 2014. “Using Sedimentological Prior  
519 Information to Control Realism in Reservoir Models”, Journal of Petroleum Technology; 66(9):38-  
520 40.
- 521 38. Rojas, T.A., Demyanov, V., Christie, M., Arnold, D. 2014. “Controlling the Sedimentological  
522 Realism of Deltaic Reservoir Models by the Use of Intelligent Sedimentological Prior Information”,  
523 First Break; 32(10):69-72.
- 524 39. Rojas, T.A., Demyanov, V., Christie, M., Arnold, D. 2013. “Learning Uncertainty from Training  
525 Images for Reservoir Predictions”, Mathematics of Planet Earth, Lecture Notes in Earth System  
526 Sciences 2014, pp 147-151. Sarma, P., Durlofsky, L.F., Aziz K. 2008. “Kernel Principal Component

- 527        Analysis for Efficient, Differentiable Parameterization of Multipoint Geostatistics”, *Mathematical*  
528        *Geosciences*, 40(1), pp. 3-32.
- 529    40. Scheidt C, Caers J. 2009. “Representing spatial uncertainty using distances and kernels”,  
530        *Mathematical Geosciences*, 41 (4), 397-419.
- 531    41. Schoelkopf, B. and Smola, A. 2002. “Learning with Kernels”. MIT Press, Cambridge MA.
- 532    42. Schulze-Riegert, R. W., Axmann, J. K., Haase, O., Rian, D. T., & You, Y. L. 2002. “Evolutionary  
533        algorithms applied to history matching of complex reservoirs”. *SPE Reservoir Evaluation and*  
534        *Engineering*, 5(02), 163-173.
- 535    43. Sonnenburg, S., Ratsch, G., Schöfer, C. and Scholkopf, B. 2006. “Large scale multiple kernel  
536        learning”, *Journal of Machine Learning Research* 7:1531–1565.9:2491–2521.9:2491–2521.
- 537    44. Strebelle, S. 2002.” Conditional Simulation of Complex Geological Structures Using Multiple-Point  
538        Statistics”. *Mathematical Geology*, 34 (1), 1-21.
- 539    45. Strebelle, S. and Zhang, T. 2005. “Non-stationary multiple-point geostatistical models”, in  
540        *Geostatistics Banff 2004*, edited by O. Leuanthong, and C. V. Deutsch, Springer, pp. 235–244.
- 541    46. Takashima, R., Tetsuya, T., Yasuo, A. 2011. “Feature selection based on multiple kernel learning  
542        for single-channel sound source localization using the acoustic transfer function”, *Acoustics,*  
543        *Speech and Signal Processing (ICASSP)*, IEEE.
- 544    47. Tsamardinos I., and Constantin F. A. 2003. “Towards principled feature selection: Relevancy,  
545        filters and wrappers”, *Proceedings of the ninth international workshop on Artificial Intelligence*  
546        *and Statistics*. Morgan Kaufmann Publishers: Key West, FL, USA.
- 547    48. Tuia, D., Camps-Valls, G., Matasci, G., Kanevski, M. 2010. “Learning relevant image features with  
548        multiple-kernel classification”, *IEEE Transactions on Geoscience and Remote Sensing*, 48: 3780-  
549        3791.
- 550    49. Vapnik, V. 1995. “The Nature of Statistical Learning Theory”. Springer-Verlag Berlin.

551 10 ANNEX

552 Geostatistical formalism

553 Conventional kriging family of algorithms accommodates hard conditioning data  $Z(\mathbf{x}_i)$  through a linear  
554 regression, which provides unbiased estimate with a minimum variance around the mean of  $Z(\mathbf{x})$   
555 (Matheron, 1969):

556 
$$Z(x) = \sum_{i=1}^N w_i Z(\mathbf{x}_i) \quad (\text{A.1})$$

557 where the regression weights  $w_i$  are computed based on the spatial correlation modelled with two-point  
558 statistics (covariance or variogram).

559 Multi-point statistics simulations generally use training images as a source of higher-order statistics  
560 spatial correlation model and provide a probabilistic estimate of a spatial random variable  $A_k$ , which can  
561 be written in a similar linear weighting form:

562 
$$P(A_k | Z(\mathbf{x}_i)) = E\{A_k\} + w \cdot (1 - E\{D\}) \quad (\text{A.2})$$

563 where  $w$  is the weight derived based on the probability of  $A_k$  according to the statistics of the data events  
564 ( $D$ ) distribution from the training image (multi-point statistics) (Marithoz & Caers, 2014). This  
565 generalised formulation becomes of kriging regression type (A.1) in a special case with two-point  
566 statistics.

567

568 11 LIST OF FIGURES

569 Figure 1. Workflow chart for MKL training for reservoir property prediction based on multiple input  
570 data: well observations, seismic and prior geological scenarios.

571 Figure 2. SVR first maps the data into the Hilbert space where linear regression is achievable; Support  
572 vectors are drawn with circles, while the crosses correspond the rest of the data (figure from Foresti et  
573 al., 2011).

574 Figure 3: Permeability realisations from the prior ensemble (sandy shelf layer).



575 Figure 4. Pressure (a) and oil saturation (b) differences obtained from 4D seismic.

576 Figure 5. MKL porosity predictor with 106 inputs – 104 prior geological realisations and 2 seismic  
577 attributes (4D pressure and saturation differences)

578 Figure 6. MKL porosity prediction maps computed with different hyper-parameter values (sandy shelf  
579 layer)

580 Figure 7. Evolution of MKL tuning parameters – kernel width  $\sigma$  – for different reservoir zones: (a)  
581 fluvial, (b) lower shore face, (c) upper shore face, (d) sandy shelf.

582 Figure 8. History matches of MKL model to production data (♦ dots) with PSO: field oil production  
583 rate (a); individual well (Pro-15) production rate (b); misfit evolution through history matching with  
584 PSO (c).

585 Figure 9. Comparison of the history match quality at individual wells between three methods: a) MKL  
586 model with PSO HM (this paper); b) kernel PCA model with PSO HM and c) EnKF history matching  
587 (after Mohamed et al., 2010 b), – green circles label good match, orange circles label fair match, red  
588 circles label poor match.

589 Figure 10. Seven selected input features for the fluvial layer (prior realisations, middle) by MKL and  
590 their corresponding weights (bar chart above) and the resulting MKL porosity prediction (bottom)

591 Figure 11. Spatial scale represented by each of the seven selected features for the fluvial layer (prior  
592 realisations) with the corresponding MKL weights (bottom)

593 Figure 12. Variogram analysis of the selected input features: omnidirectional variograms for the seven  
594 selected input features represent different spatial correlation scale; bottom right – spatial anisotropy  
595 (geometrical) direction according to the variogram ranges of the three features (from the selected seven)  
596 with the corresponding MKL weights, spatial correlation for the rest four selected realisations is  
597 isotropic

598 Figure 13. Variation of the contribution of a selected input features across multiple HM models  
599 obtained from 20 runs: three features, which represent different spatial scales, were selected in each of  
600 the 20 HM matches, but the weight of their contribution varies from one HM to another.

601

Figure(s)

[Click here to download high resolution image](#)

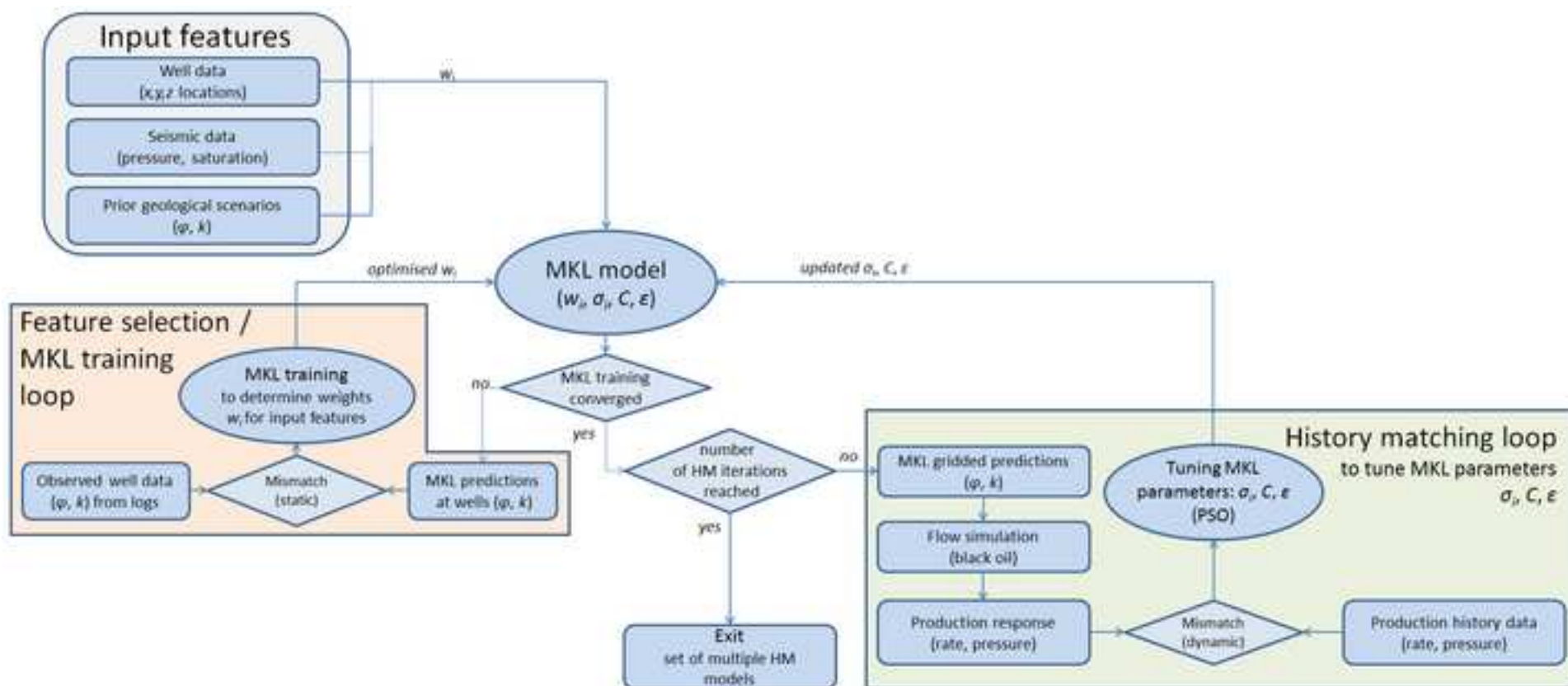
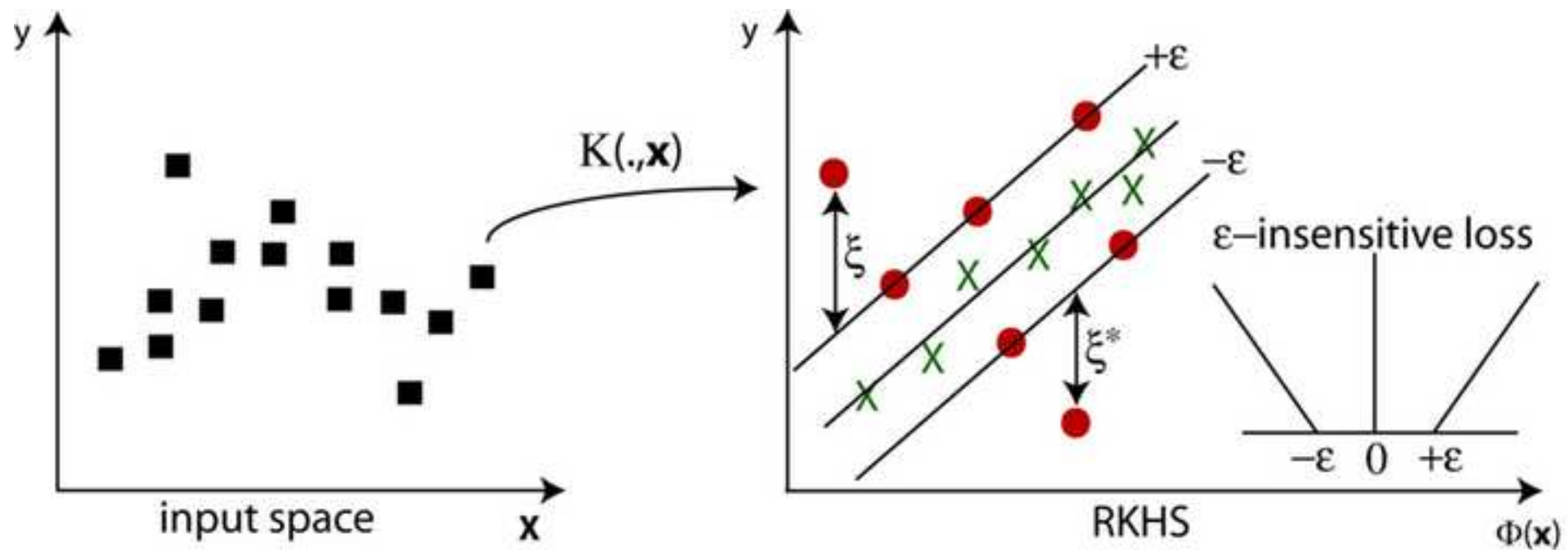
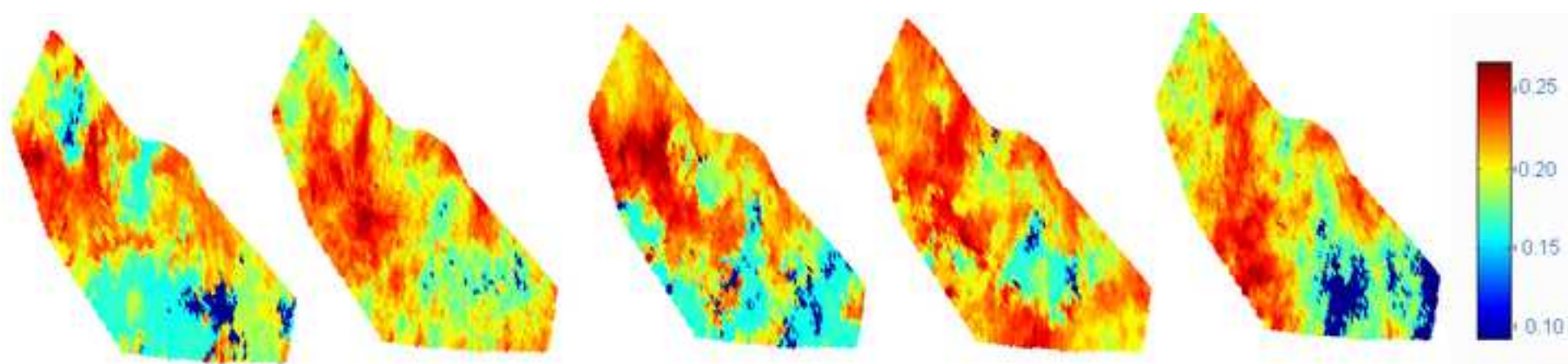


Figure 2  
[Click here to download high resolution image](#)



**Figure 3**  
[Click here to download high resolution image](#)



**Figure 4**  
[Click here to download high resolution image](#)

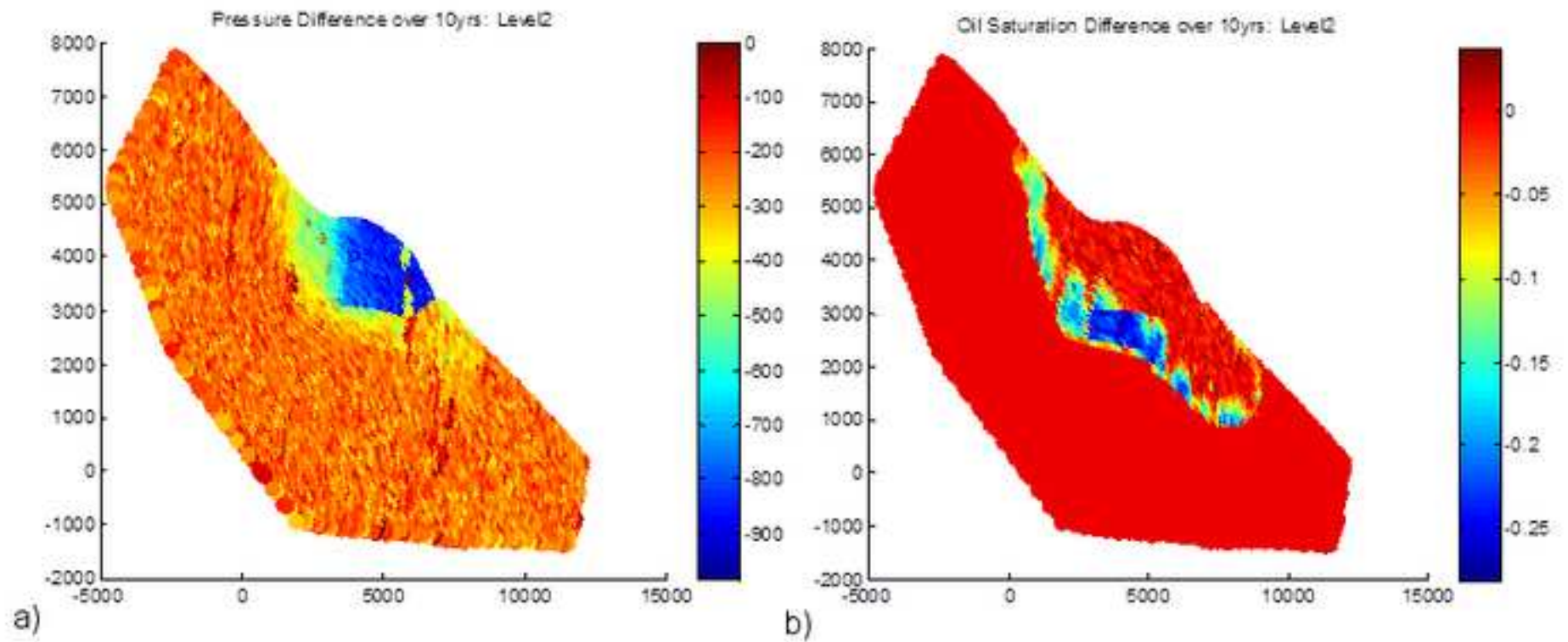
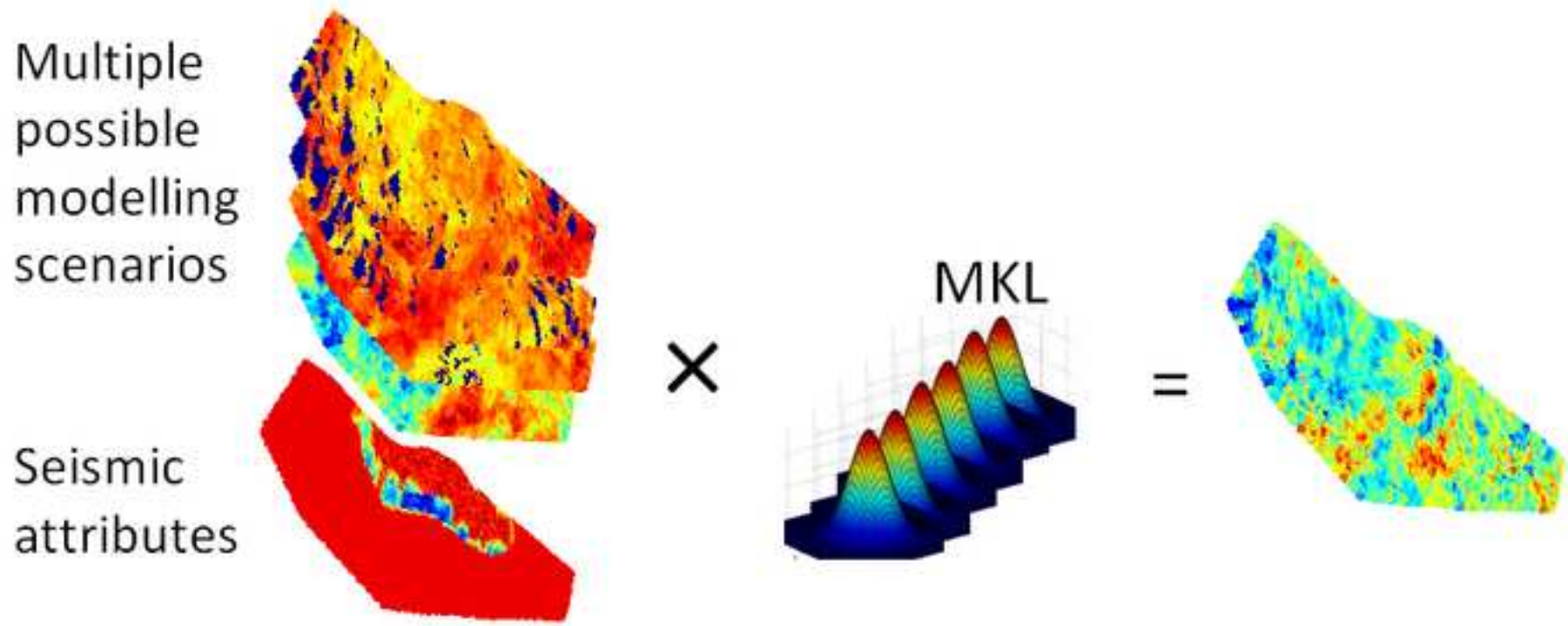


Figure 5  
[Click here to download high resolution image](#)



**Figure 6**  
[Click here to download high resolution image](#)

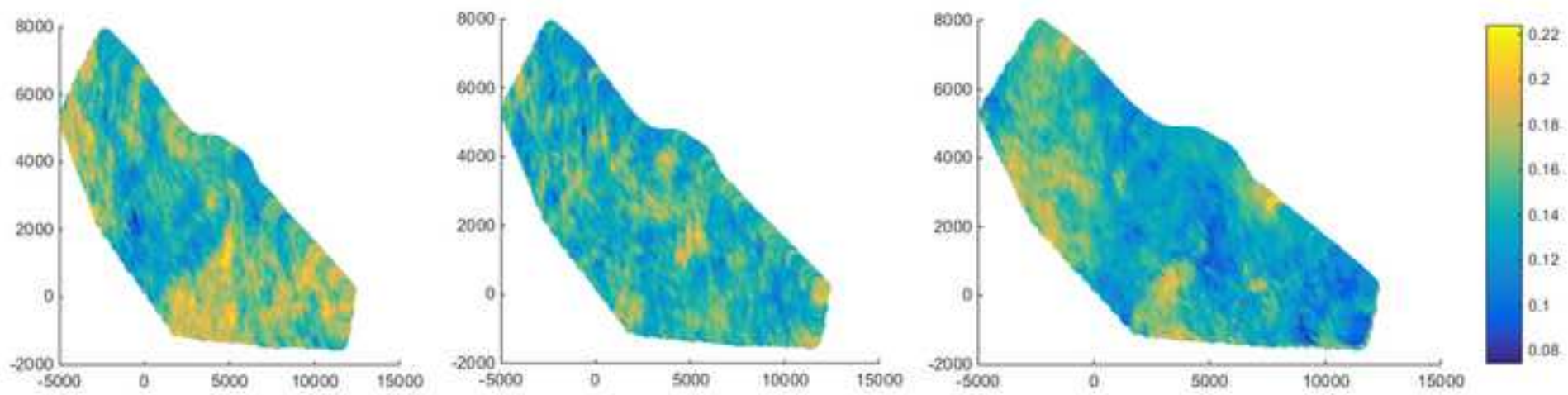




Figure 7  
[Click here to download high resolution image](#)

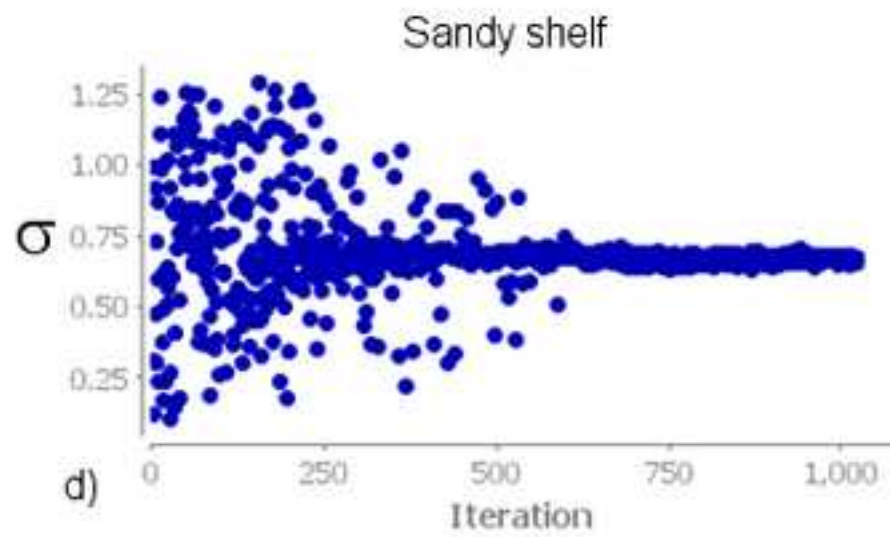
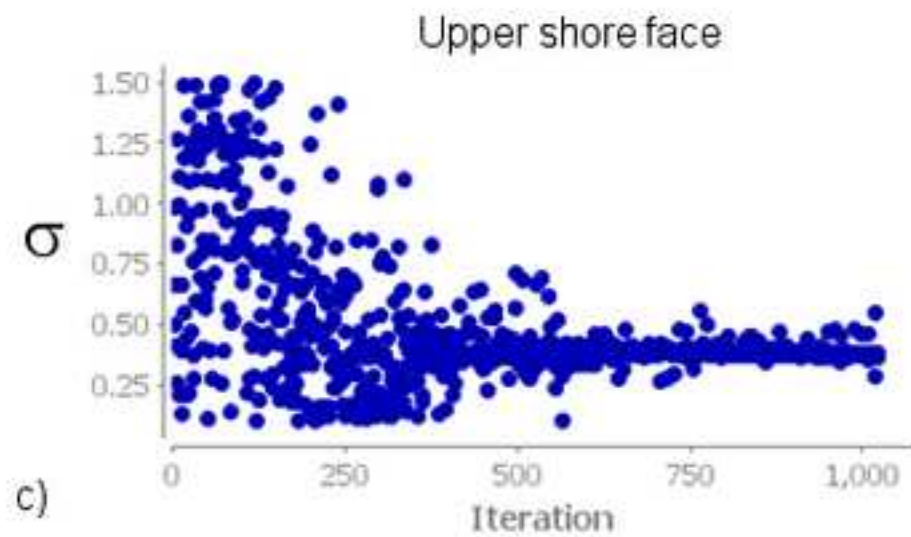
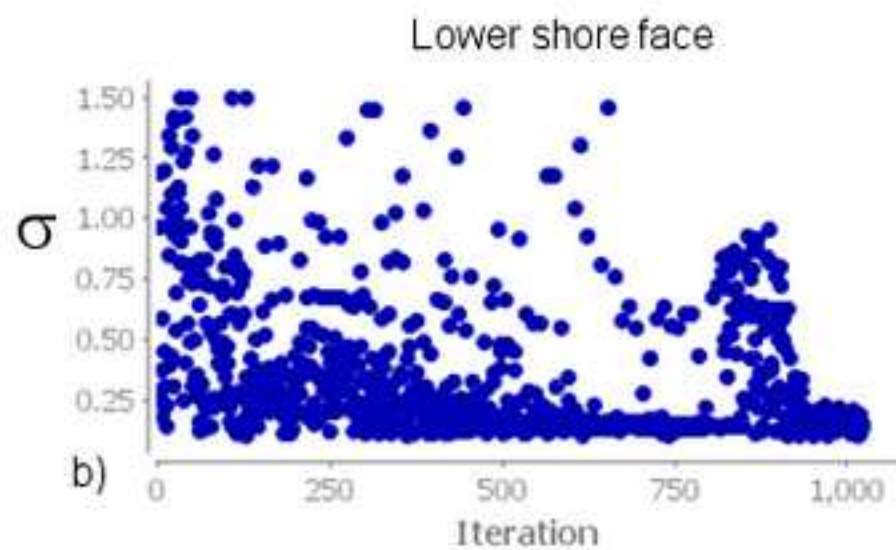
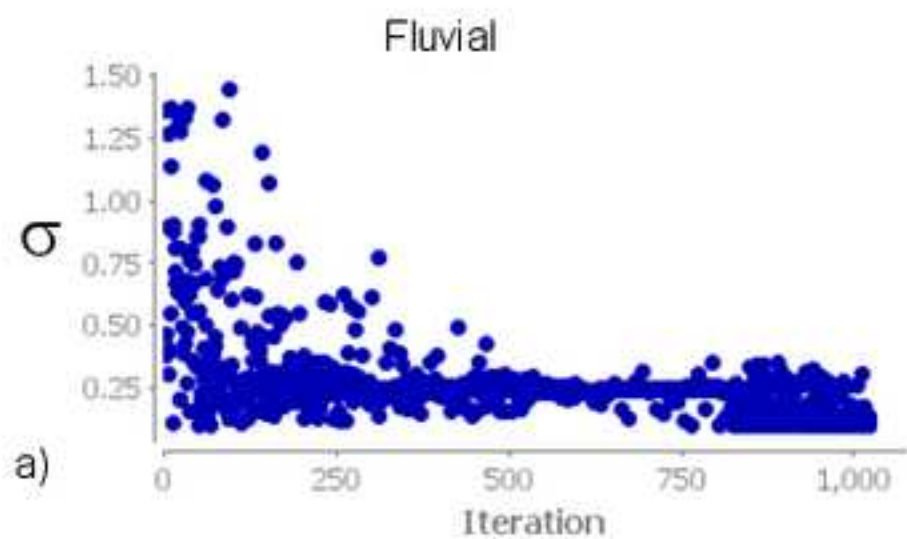


Figure 8a  
[Click here to download high resolution image](#)

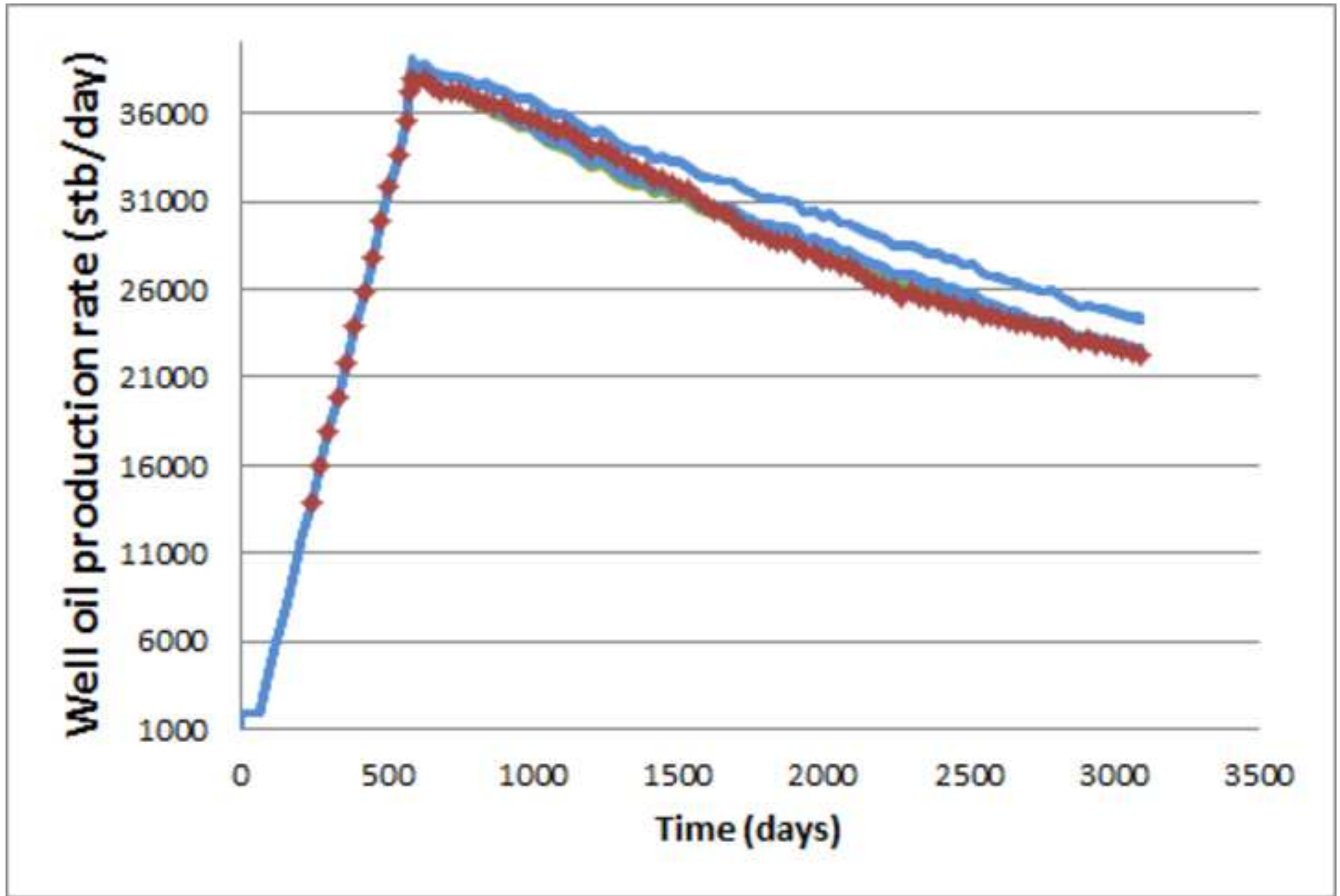


Figure 8b  
[Click here to download high resolution image](#)

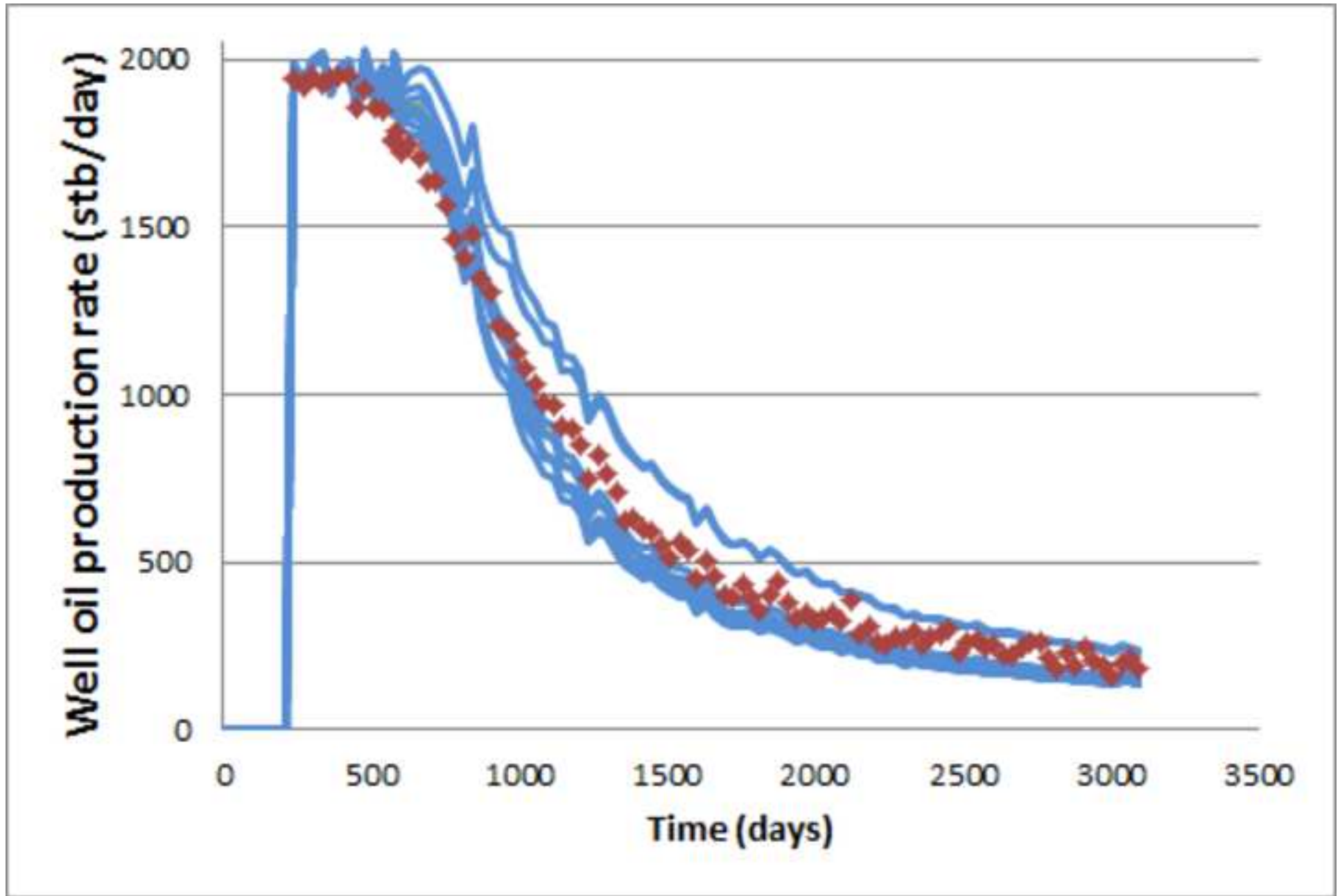


Figure 8c  
[Click here to download high resolution image](#)

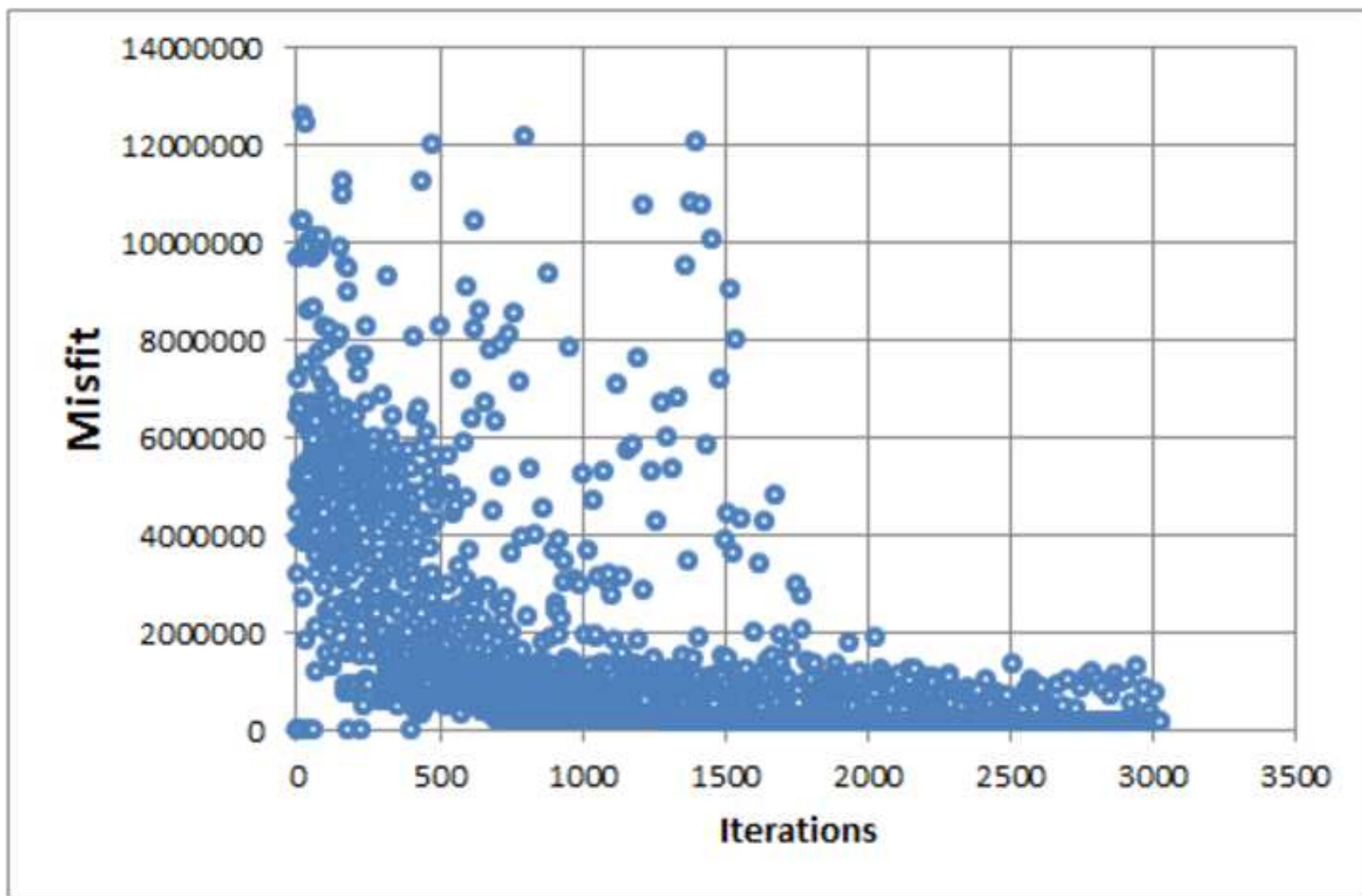


Figure 9a  
[Click here to download high resolution image](#)

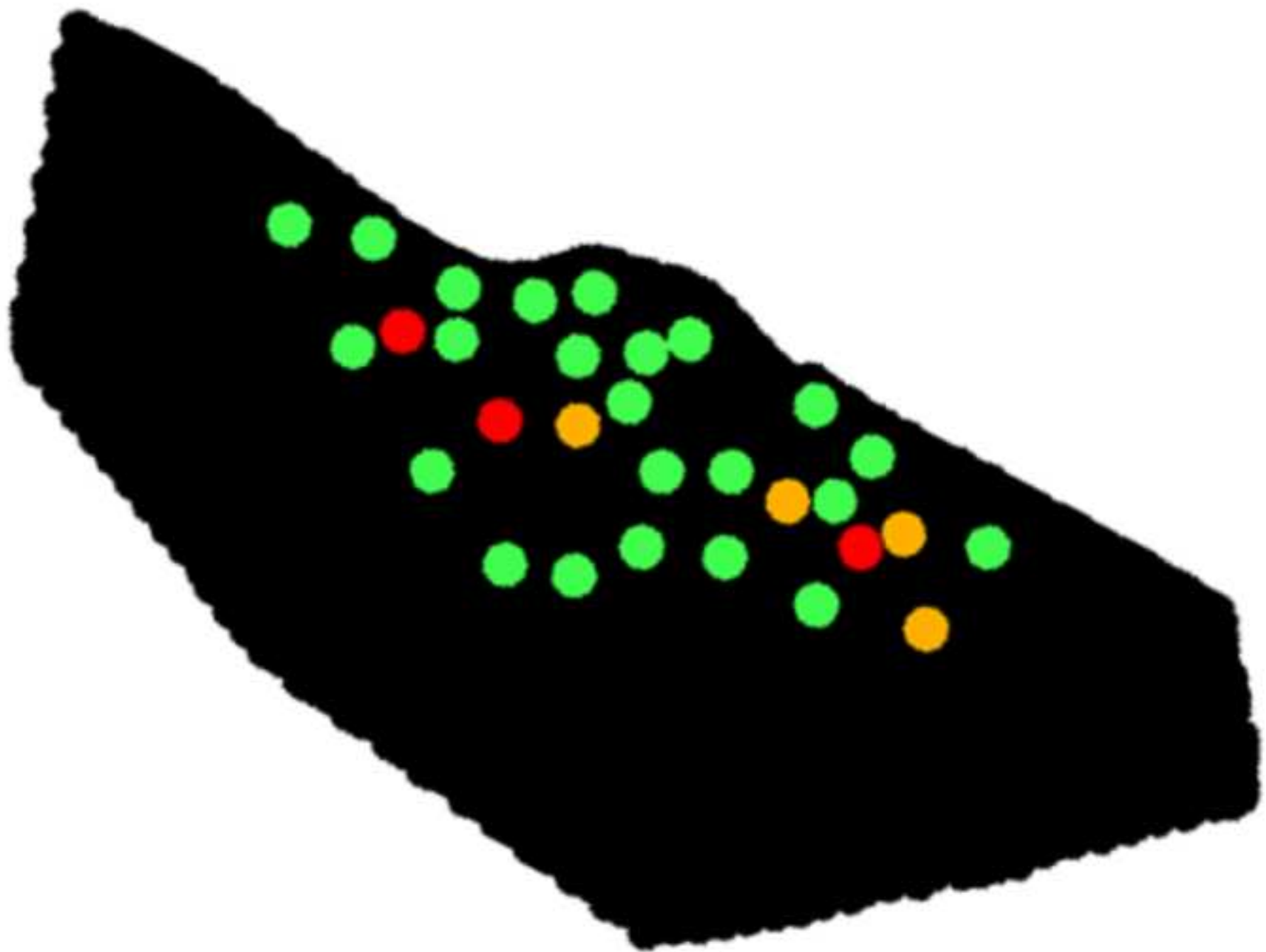


Figure 9b  
[Click here to download high resolution image](#)

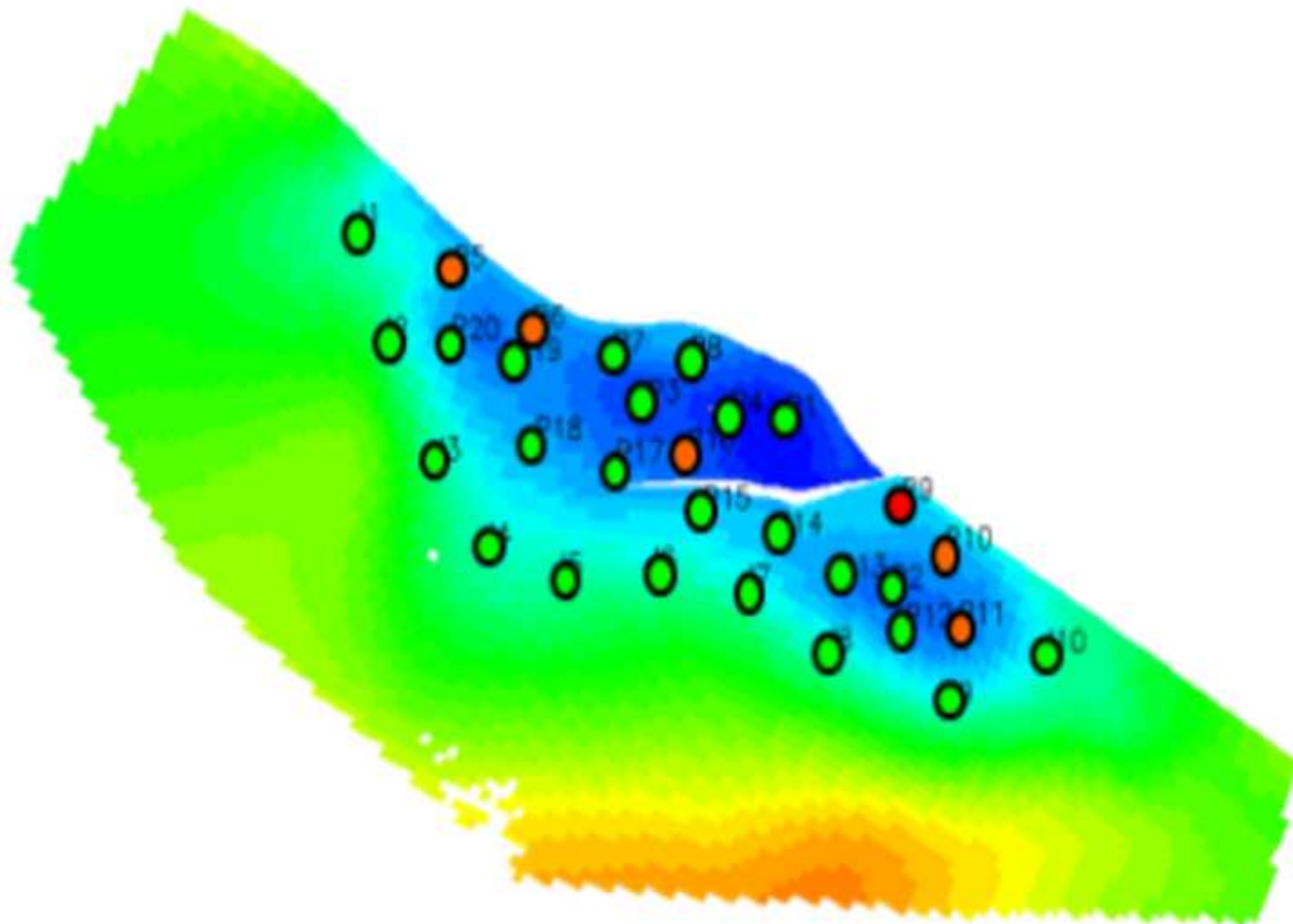


Figure 9c  
[Click here to download high resolution image](#)

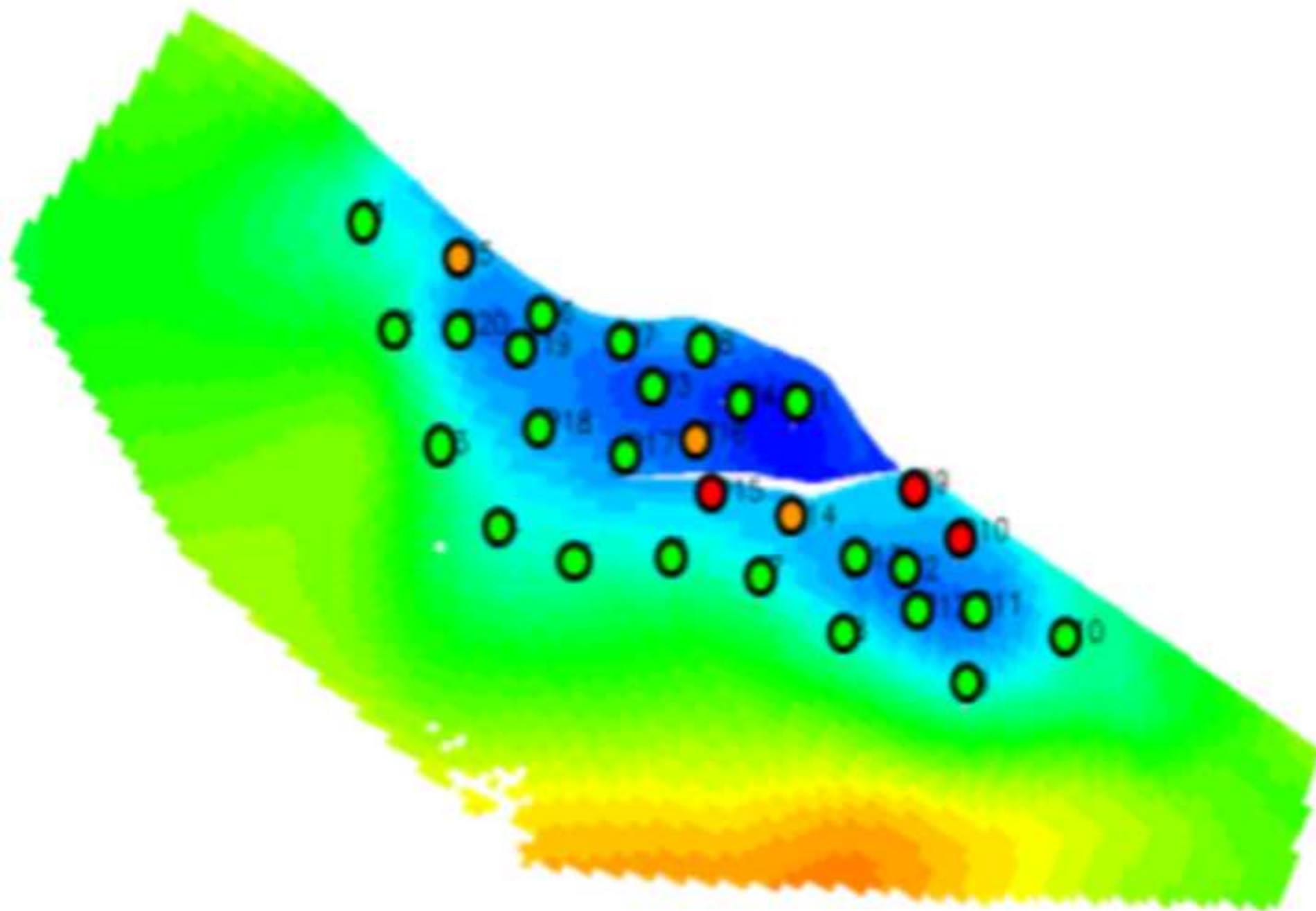


Figure 10  
[Click here to download high resolution image](#)

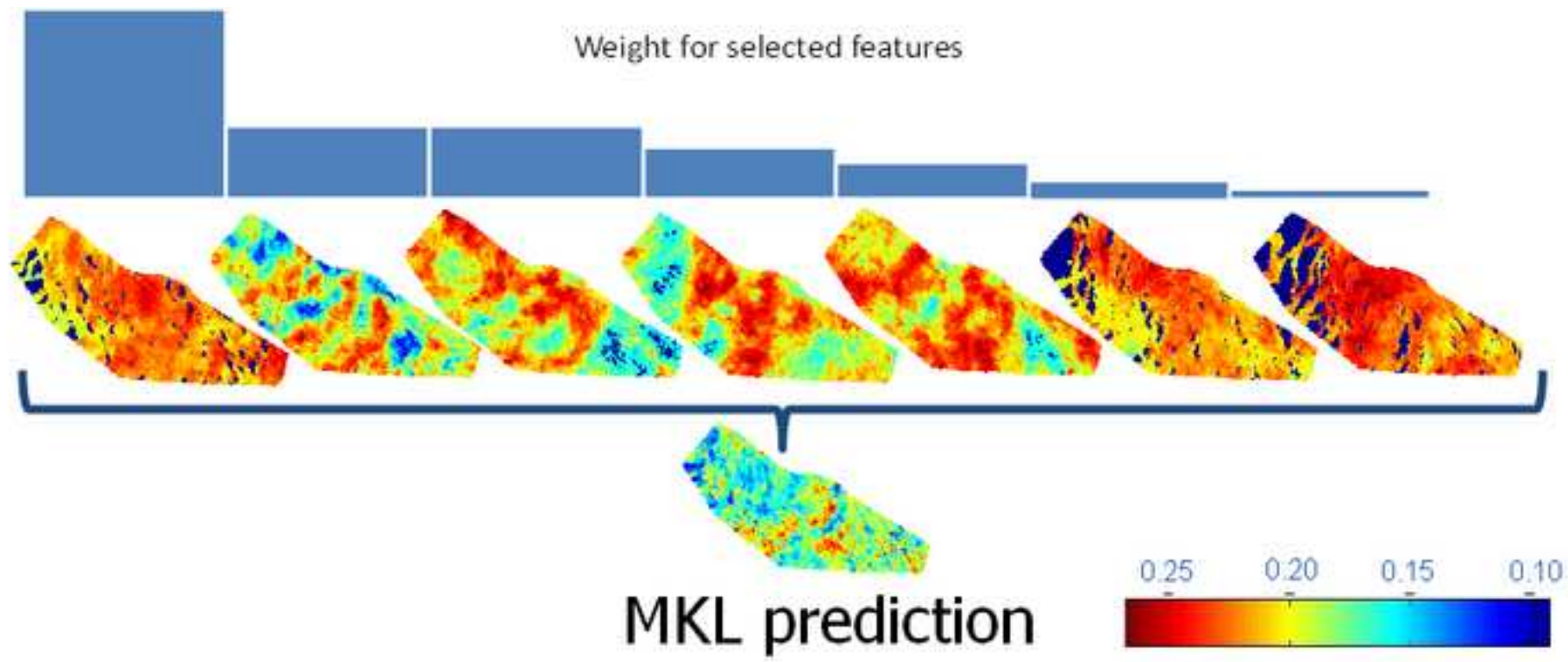




Figure 11

[Click here to download high resolution image](#)

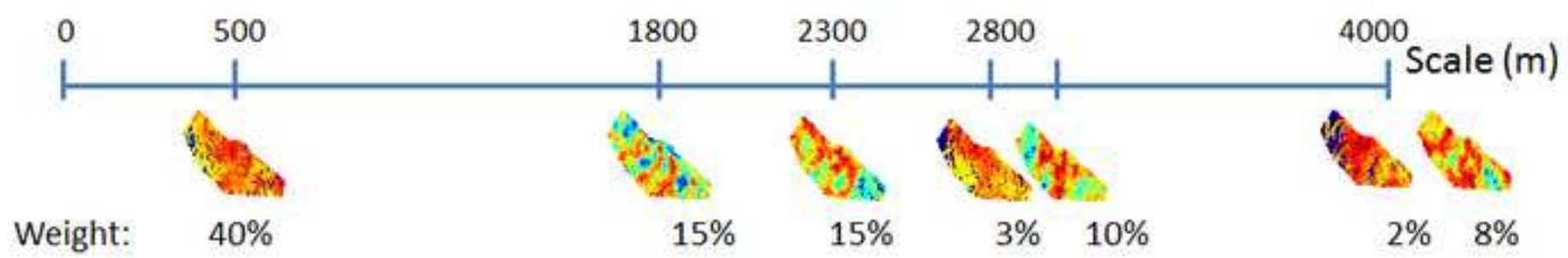


Figure 12  
[Click here to download high resolution image](#)

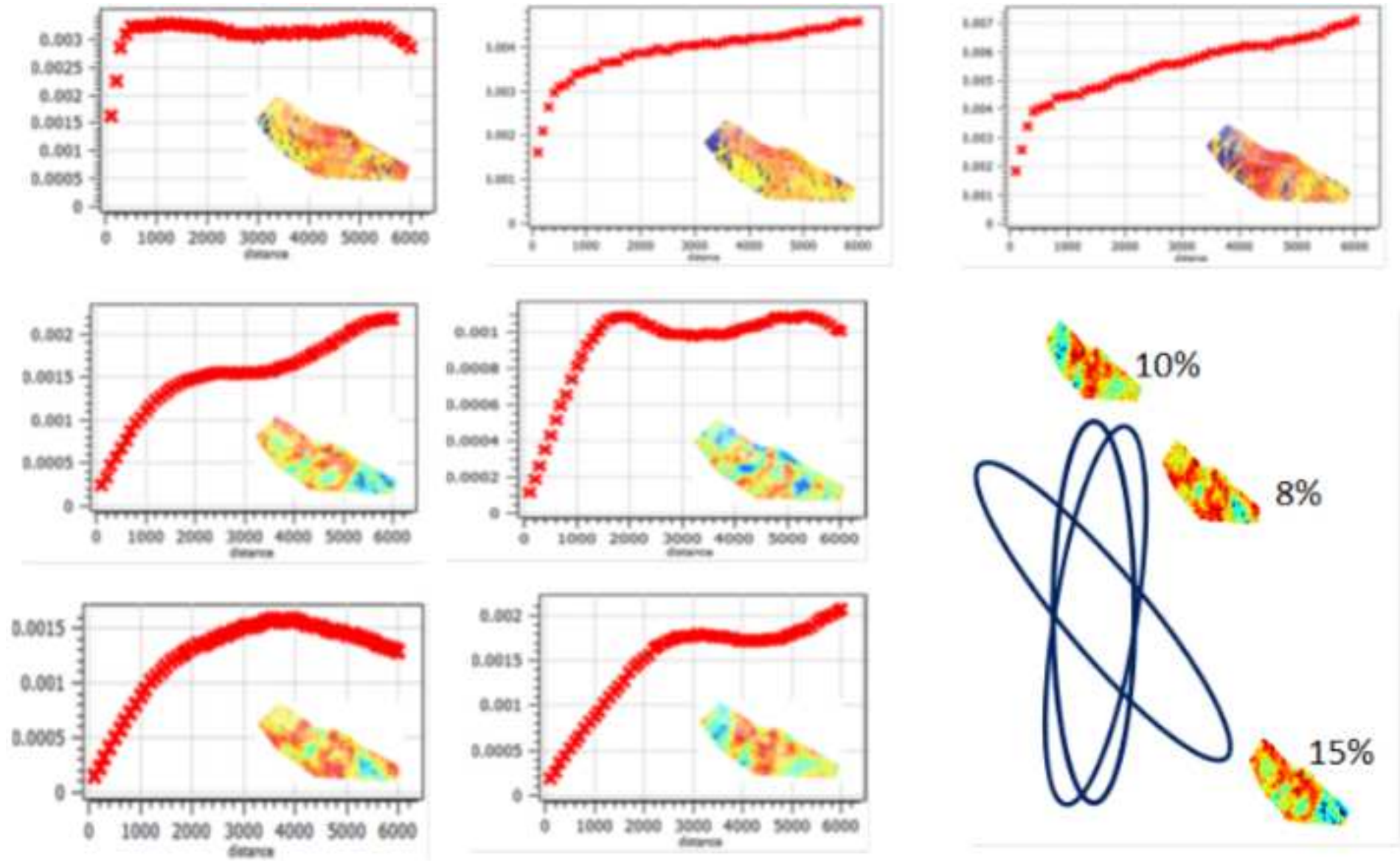


Figure 13  
[Click here to download high resolution image](#)

